CNWRA *A center of excellence in earth sciences and engineering*

A Division of Southwest Research Institute™
6220 Culebra Road • San Antonio, Texas, U.S.A. 78228-5166
(210) 522-5160 • Fax (210) 522-5155

October 27, 2000
Contract No. NRC–02–97–009
Account No. 20.01402.571

U.S. Nuclear Regulatory Commission
ATTN: Mrs. Deborah A. DeMarco
Two White Flint North
11545 Rockville Pike
Mail Stop T8 A23
Washington, DC 20555

Subject: Programmatic Review of Paper

Dear Mrs DeMarco:

Enclosed is a paper entitled "Long-Term Dissolution of Alloy 22: Experiments and Modeling," to be presented at the Corrosion 2001 Conference on March 11–16, 2001 in Houston, Texas. The paper describes both experimental and modeling work performed to date to address the uncertainties associated with predicting the long-term performance of waste package outer container in the absence of localized corrosion and stress corrosion cracking. Please advise me of the results of your programmatic review, so we can submit the paper for publication in a timely manner.

If you have any questions regarding this paper, please feel free to contact Darrell Dunn at (210) 522-6090 or Sean Brossia at (210) 522-5797.

Sincerely yours,

Budhi Sagar
Technical Director

DSD:ph

Enclosure

cc: J. Linehan, B. Meehan, E. Whitt, T. Essig, J. Contardi, T. Bloomer, T. Ahn, K. Stablein, J. Greeves, J. Thomas, J. Holonich, B. Leslie, C. Greene, J. Andersen, W. Patrick, CNWRA EMs, CNWRA Dirs., S. Brossia, O. Pensado, G. Cragnolino, P. Maldonado, T. Nagy (contracts)

Washington Office • Twinbrook Metro Plaza #210
12300 Twinbrook Parkway • Rockville, Maryland 20852-1606

CORROSION 2001 paper #125

Long-Term Dissolution Behavior of Alloy 22: Experiments and Modeling

D.S. Dunn, C.S. Brossia, O. Pensado
Center for Nuclear Waste Regulatory Analyses
Southwest Research Institute
6220 Culebra Road
San Antonio, TX 78238-5166

ABSTRACT

The long-term integrity of containers for the disposal of high-level nuclear waste in the absence of environmental conditions leading to localized corrosion and stress corrosion cracking is based on the assumption that passive dissolution of Alloy 22 is the dominant mechanism. Corrosion rate measurements under passive and transpassive conditions were performed as a function of temperature, solution pH, and chloride concentration. Analyses of solutions using capillary electrophoresis and the corrosion product deposit using SEM-EDS were performed in order to determine if dissolution was stoichiometric or if preferential dissolution of certain alloying elements was favored. Preliminary measurements suggest that under passive conditions, the dissolution rate is low and stoichiometric. Modeling of passive film dissolution also suggests that while preferential dissolution can occur in the short term, long-term dissolution is likely to be stoichiometric.

INTRODUCTION

Waste packages manufactured from corrosion resistant materials are presently being evaluated for the permanent disposal of high-level nuclear waste in the proposed repository at Yucca Mountain (YM) Nevada. The waste packages must be resistant to localized corrosion, stress corrosion cracking, and mechanical degradation as a result of rockfall or seismic events in order to provide long term isolation of the radioactive materials form the accessible environment[1]. At present, the proposed waste package design uses a 50 mm thick type 316 nuclear grade (NG) inner container to provide mechanical strength and a 20 mm thick Alloy 22 outer container to provide localized corrosion and stress corrosion cracking resistance.

The degradation of Alloy 22 is expected to occur by passive dissolution and delay penetration of the outer corrosion resistant barrier for many thousands of years. As a result, a low rate of passive dissolution of the outer barrier is a necessary requirement to achieve long term isolation of the radionuclides. Aside from the initiation of localized corrosion, stress corrosion cracking, and loss of ductility and corrosion resistance as a result of phase instability, changes in both the structure and the composition of the passive film on Alloy 22 may also decrease the expected lifetime of the outer corrosion resistant barrier. Alteration of the passive film

chemical composition may occur over long periods as a result of selective dissolution. Changes in the passive film structure may occur through the formation and accumulation of vacancies arising from the passive dissolution of the alloy.

Many investigations have focused on the formation and compositional evolution of passive films[2-10]. On Fe-Cr and Ni-Cr alloys, passive films tend to be enriched in Cr suggesting the preferential dissolution of Fe and Ni from the oxide layer. Analyses of the passive films on Fe-Cr, Fe-Cr-Ni-Mo, alloys suggest the presence of an inner layer composed of mainly Cr_2O_3 and an outer layer composed of chromium hydroxides[5,10] Haupt and Strehblow[4] analyzed the passive layers on Fe-15Cr using XPS and found that alloy specimens passivated for times up to 1 week at 0.9 V_{SCE} in 0.5 M H_2SO_4 contain up to 70 percent Cr as a result of preferential dissolution of Fe. Olefjord and Wegrelius[5] examined the passive films formed on Fe-20Cr-18Ni-6Mo-0.2N stainless steel in 0.1 M HCl + 0.4 M NaCl solution at potentials in the range of -0.1 to 0.5 V_{SCE}. The passive film was observed to be composed of an inner Fe and Cr rich oxide and a outer $Cr(OH)_3$ layer. The oxide layer thickness increased with potential whereas the hydroxide layer thickness was independent of potential. Both Cr and Mo were enriched in the oxide and hydroxide layers. Increasing the potential was observed to decrease the Cr and Mo concentrations and increase the Fe concentration in the inner oxide layer.

Analyses of Ni-Cr, Ni-Cr-Fe and Ni-Cr-Mo alloys have shown an inner layer composed of mainly Cr_2O_3 and an outer layer of nickel oxides[2,3,6], similar to the results obtained on Fe-Cr alloys. Marcus and Grimal[2] used X-ray photoelectron spectroscopy (XPS) to examine the passive film formation on Ni-21Cr-8Fe in 0.05 percent H_2SO_4 and found that the inner oxide layer contained as much as 96 percent Cr_2O_3 and 4 percent Fe_2O_3. Boudin et al.[3] reported significant enrichment of Cr in the oxide layer of Ni-Cr alloys analyzed using Auger electron spectroscopy (AES) and low energy ion scattering spectroscopy (LEIS) . For alloys containing at least 17 percent Cr, the inner oxide layer was observed to have up to 80 percent Cr. Lorang et al.[6] reported that the distribution of elements in the passive films of Alloy C-4 also show an increased Cr concentration in the oxide film compared to the bulk alloy indicating that the behavior of Ni-Cr-Mo alloys is quite similar to the Fe-Cr alloys. The maximum chromium concentration was observed when the alloy was passivated at -0.2 V_{SCE} in 5 M NaCl at 20°C for 2 hours. Increasing the applied potential decreased the chromium concentration and increase the chloride concentration in the passive layer. In contrast alloys passivated at 90°C had higher Cr concentrations, which may be attributed to the faster dissolution rate of Ni and Mo at elevated temperatures. The Mo concentration of the passive layer was much lower than that in the bulk alloy. Somewhat contradictory results were reported by Cavanaugh et al.[7] for Alloy C-276 in 0.5 N NaCl at 70 °C. The dissolution of Fe from Alloy C-276 was determined to be proportional to that of Ni, where as the concentrations of Cr and Mo in the solution were less than the comparable concentrations of the elements in the alloy. As the potential was increased the relative dissolution of both Mo and Cr increased, however even under transpassive conditions (950 mV_{SCE}) the dissolution of Cr was observed to be less than stoichiometric.

The composition of the oxide film has also been related to the rate of passive dissolution. Yang et al.[8] measured decreasing passive current densities and increasing Cr(III) concentrations in the oxide film of a Fe-17 Cr alloy aged at 0.390 V_{SHE} in solutions containing 0.02 M chloride. Kirchheim and coworkers[9-12] conducted a series of investigations focused on compositional changes in the passive layers and their relation to passive dissolution rate for a variety of alloy systems. Heine and Kirchheim[9] and Kirchheim et al.[10] calculated the dissolution current density of Fe-Cr alloys in 1 N H_2SO_4 by measuring the concentrations of Fe and Cr in solution using atomic absorption spectroscopy. Passive current densities decreased as the Cr concentration in the alloy increased. The passive current density for a 15 percent Cr alloy after a 96 hour exposure was 0.06 $\mu A/cm^2$. A lower passive current density of 0.014 $\mu A/cm^2$ was measured for pure Cr. Analysis of the oxide films using XPS indicates that Cr enrichment was observed for all Cr containing alloys with the oxide of the Fe-18 Cr alloy having 58 to 65 atomic percent (cation) Cr.

The objectives of this investigation were to measure the passive corrosion rates using electrochemical

methods and determine whether the dissolution is stoichiometric or nonstoichiometric under passive and transpassive conditions. In addition, tests were also designed to provide experimental data to model the formation of the oxide film under passive conditions.

EXPERIMENTAL METHODS

The chemical composition of the Alloy 22 heat used in this investigation is shown in Table 1. Prior to the start of a test, all specimens were polished to a 600 grit finish, cleaned ultrasonically in detergent, rinsed in deionized (DI) water, ultrasonically cleaned in acetone, and dried. Passive dissolution rates were measured in solutions containing 0.028 to 4.0 M NaCl under potentiostatic polarization. Tests were conducted in a 2-L glass cell with a PTFE lid. The cells were fitted with a water-cooled Allihn-type condenser and a water trap to minimize solution loss at elevated temperatures and air intrusion. A saturated calomel electrode (SCE) was used as a reference electrode in all experiments. The SCE was connected to the solution through a water-cooled Luggin probe with a porous silica tip so that the reference electrode was maintained at room temperature. A platinum flag was used as a counter electrode. All solutions were deaerated with high-purity nitrogen (99.999 percent) for a period of at least 24 h prior to the start of the tests in order to obtain accurate anodic current density measurements at potentials ranging from −200 to 800 mV_{SCE}. Specimens were held potentiostatically for a period of 48 hr while the anodic current density was recorded. The resolution of the current measurement was determined to be 1.25×10^{-10} A/cm^2. At the conclusion of the test, the specimens were reweighed and examined microscopically for signs of corrosion.

Corrosion rates were calculated using Eq. (1)

$$CR\,(mm/yr) = \frac{K\, i_{corr}\, EW}{\rho} \qquad (1)$$

where i_{corr} is the passive corrosion current density in A/cm^2, EW is the equivalent weight, K is a conversion factor (3,270 mm·g·A^{-1}·cm^{-1}·yr^{-1}) and ρ is the density in g/cm^3. For Alloy 22, ρ is 8.69 g/cm^3. Assuming congruent dissolution of the major alloying elements as Ni^{2+}, Cr^{3+}, Mo^{3+}, Fe^{2+}, and W^{4+} within the potential range of −200 to 400 mV_{SCE}, the EW for Alloy 22 is 26.04 g/equivalent[13].

Soluble corrosion products formed during passive dissolution were analyzed using Capillary Electrophoresis (CE). In CE, ionic speciation is achieved based on differences in the ionic migration time of the species present in the unknown solution under an applied electric field, in this case 20 kV. Species are then detected as they pass a UV lamp/detector assembly. Quantitation is performed by comparison of peak areas to those measured on samples of known concentration. Samples were loaded into the capillary using hydrostatic sampling for 30 s at a height of 10 cm. This sampling method roughly amounts to a sampling volume of 37 nL using a 75 µm ID capillary. All oxyanions (CrO_4^{2-}, MoO_4^{2-}, WO_4^{2-}) were detected directly using a 214 nm lamp and the method described by Kelly et al.[14] in which the capillary electrolyte consisted of deionized water with 1.5 mM Na_2SO_4, 2.5 mM osmotic flow modifier Anion BT and pH adjusted to 10.5 using NaOH. All cations (K^+, Na^+, Cr^{3+}, Ni^{2+}) were analyzed using the method described by Krol et al.[15] using indirect detection at 254 nm and a capillary electrolyte consisting of deionized water with 6 mM benzimidazole, 2.5 mM tartaric acid, and 2 mM 18-crown-6-ether. All samples were analyzed at 25 °C with a nominal minimum detection limit of ~ 70 to 100 ppb for all species of interest. Tests were conducted in 220 to 250 mL of deaerated 0.028 M KCl solutions. Initial analyses of test solutions using CE were performed using small specimens with an area of 8 cm^2. Subsequent tests were performed using a specimen with a surface area of 72 cm^2. Specimens were held potentiostatically for a period of 330 hr in a test cell equipped with provisions for extracting small samples of solution for analyses.

RESULTS

The results of passive current density measurements obtained after 48 hr under potentiostatic conditions are shown in Figure 1. At potentials of 200 mV_{SCE} or less, the passive current was in the range of 6×10^{-9} to 3×10^{-8} A/cm^2 and was relatively independent of the chloride concentration and solution pH in the range of 2.7 to 8.0. In tests conducted at potentials above 400 mV_{SCE}, the onset of transpassive dissolution was observed. At pH 0.7 the passive current densities increased to approximately 7×10^{-8} A/cm^2 at 200 mV_{SCE}. The increase in the anodic current density observed at pH 0.7 at an applied potentials of 200 to 600 mV_{SCE} may be the result of enhanced oxide film dissolution in this highly acidic solution. Temperature, on the other hand, had a significant effect on the passive corrosion rate in dilute chloride solutions (Figure 2). The passive corrosion rate increased by a factor of 10 when the temperature of the 0.028 M chloride solution (pH 8.0) was increased from 20 to 95 °C. However, practically no temperature effect was noted in 4 M chloride. Increasing temperature also decreased the potential range over which the passive film was stable. At 20 °C, passive behavior was observed at potentials just above 400 mV whereas transpassive behavior was observed at these potentials when the solution temperature was increased to 95 °C.

Initial analyses of solutions using CE were performed using a small test specimen (8 cm^2) immersed in 220 mL of solution. The specimen was potentiostatically polarized at 100 mV_{SCE} for 300 hr. After a period of 280 hours, the passive current density was in the range of 8.4×10^{-9} to 9.0×10^{-9} A/cm^2 (Figure 3). Integrating the current density with time resulted in a calculated charge density of 0.015 C/cm^2 over the duration of the test. Assuming stoichiometric dissolution, the total metal ion concentration as a result of Alloy 22 corrosion should be 147 ppb at the conclusion of the test with 84 ppb Ni and 32 ppb Cr. Analyses of the solution using CE did not detect the presence of any species expected to result from the passive dissolution.

The current density and total charge as a function of time for the transpassive dissolution of Alloy 22 are shown in Figure 4. Measured concentrations of Cr(VI), Mo(VI), W(VI) (analyzed as oxyanions CrO_4^{2-}, MoO_4^{2-}, WO_4^{2-}), and Ni^{2+} in solution as a function of time are shown in Figure 5. The calculated charge in coulombs necessary to achieve the combined concentrations of these species is shown in Figure 6. It is apparent that the charge measured by integrating the current density as a function of time (Figure 4) is more than 3 times that calculated based on the concentrations of the metal cations and oxyanions. In addition, the concentration of Ni^{2+} after an initial increase actually decreases with time. These discrepancies indicate that removal of corrosion products from the solution is occurring throughout the duration of the test. Examination of the cell after the conclusion of the test revealed the deposition of a Ni-rich precipitate on the Pt counter electrode and a deposit layer rich in Mo, W, Cr and Fe on the Alloy 22 specimen. Although the chemical composition of the deposits, determined using SEM EDS analyses are shown in Table 2, quantitative analyses of these deposits were not yet performed.

The geometry of the test specimen was changed in order to increase the surface area to solution volume ratio. The larger specimen had a surface area of 72 cm^2 and was tested under passive conditions at a potential of 0 mV_{SCE} in 0.028 M Cl^- at 95 °C. In spite of the increased surface area, no cations or oxyanions expected to occur as a result of the passive dissolution of Alloy 22 were observed after 660 hours of testing where a total charge of 1.82 coulombs (2.53×10^{-2} C/cm^2) was recorded corresponding to a total metal concentration of 2,230 ppb if no precipitation or redeposition of the cations and oxyanions occurred.

DISCUSSION

Measurement of the passive corrosion rate of Alloy 22 has been performed using electrochemical methods. Determination of the extent of preferential dissolution of alloying elements from the passive film was

attempted; however, the combination of a less than optimized cell geometry, limited resolution of the solution chemistry analyses, and the deposition of corrosion products prevented a clear assessment of the nature of the passive dissolution process. Analyses of solutions indicate the dissolution of Cr is approximately stoichiometric under transpassive conditions. Additional tests, performed using a modified arrangement to optimize the test cell geometry are being conducted to attain an understanding of the passive dissolution of Alloy 22

If localized corrosion is not initiated and the corrosion potential of Alloy 22 is lower than 400 mV_{SCE}, the lifetime of the alloy can be predicted[16] from the potentiostatic measurements of the passive current density and the application of Faraday's laws according to Eq. (1). For example, it can be estimated that the life of a 2-cm thick wall of alloy 22 under passive dissolution is of the order of tens of thousands of years[17]. This estimate, relevant to the performance of high-level waste containers in the proposed repository at Yucca Mountain, relies on two hypothesis: stoichiometric and homogeneous dissolution. In this paper, "homogeneous dissolution" is referred to dissolution phenomena not resulting in the creation of defects in the bulk of the alloy. These two hypothesis are analyzed with the support of a mechanistic model[18,19] based on the point defect model[20].

The model is intended to describe the passive dissolution of Ni-Cr-Mo alloys. The passive dissolution in alloy 22 is assumed to be controlled by the formation of a protective Cr_2O_3-rich film on the metal surface, based on observations by Boudin et al.[3] for other Ni-Cr alloys in which the Cr content is greater than 12 to 15 wt%. It is assumed that the conduction mechanism through the Cr_2O_3 film is mainly by interstitial cations or oxygen vacancies or by both carriers, implying a steady-state passive current density independent of potential. Cation vacancies are the carriers in the NiO film on pure Ni[20], which exhibits a passive current density that increases exponentially with potential[21]. It is assumed that the Cr_2O_3 film, lacking relevant proportions of Mo, contains Cr, Ni, and Mo as interstitial defects, Ni as a substitutional defect, and oxygen and Cr vacancies. Based on the observation that the passive current density decreases with increasing Cr content in Ni-Cr alloys, it can be demonstrated that, in the relatively short term, preferential dissolution of Ni occurs through the Cr-rich passive film, as reported by Cavanaugh et al.[7] As result of constraints in estimated values of rate constants for the elementary reactions associated with the creation of interstitials (Cr, Ni, and Mo) and substitutionals (Cr and Ni) at the metal/film interface, it is concluded that charge transport through the passive film is mainly due to interstitial species. Since interstitial conduction is associated with the creation of vacancies in the bulk of the alloy, the hypothesis of homogeneous dissolution needs additional evaluation.

Preliminary mass-balance computations on the effect of vacancies in the alloy lifetime have been reported elsewhere[18,19]. In these computations it has been argued that, for a plate of Alloy 22 with one surface exposed to the electrolyte, vacancies accumulate in the bulk of the alloy with negligible change in time of the plate thickness (i.e., the alloy evolves into a porous structure). Setting as failure criterion[22] the establishment of a maximum porosity, such as 50 percent,[1] results in shorter lifetimes than those predicted with the hypotheses of stoichiometric and homogeneous dissolution. The formation of porous structures is commonplace in the dealloying of binary alloys composed of a reactive element (e.g., Mg, Al, Mn, Zn) and one more noble element (e.g., Ag, Ag, Cu, Ni) and polarized at a potential above the critical potential such that the reactive component actively dissolves, but not the noble component[23,24]. Nonetheless, it is difficult to defend the notion of the evolution of alloy 22 into a porous structure at repository service conditions given the extremely low vacancy diffusivities expected at temperatures of the order of 100°C.

More refined computations accounting for finite vacancy diffusivities indicate that vacancies tend to accumulate at the metal/film interface. This accumulation could potentially lead to film spalling, in close

---

[1] Other authors have followed a similar approach to define material failure. For example Raj and Ashby (1975), in their diffusion controlled cavity growth (DCCG) model, postulate that mechanical failure for a material subject to creep occurs when the grain boundaries contain 50 percent of vacancies.

similitude to the mechanism proposed by Macdonald[20] for the onset of localized corrosion. In Macdonald's model, cation vacancies accumulate at the metal film interface, causing the oxide film to detach from the metal as a result of voids formed by coalescence of vacancies. Note that in his model, cation vacancies are defects of the oxide, and not of the bulk of the metal as in the present case. The following heuristic model is proposed to account for film spalling. A finite difference approach is implemented to track vacancy transport, which requires partitioning of the alloy plate thickness into N subdivisions as indicated in Figure 7. A vacancy concentration fraction, P, is defined as

$$P = \frac{c_v}{c_{Ni} + c_{Cr} + c_{Mo} + c_v} \tag{2}$$

where c_j are concentrations (mol/cm^3) computed in the first cell in Figure 7 (i.e., between x_0 and x_1), and the subscripts *v, Ni, Cr,* and *Mo* represent vacancies, nickel, chromium, and molybdenum, respectively. When P exceeds a critical value, P_{max}, film spalling is assumed to occur, probably followed by active dissolution of the alloy. In the heuristic model, when P exceeds P_{max} the metal/film interface is advanced to the position x_1. The time at which the thickness of the alloy slab is zero is defined as the failure time of the alloy.

Results from the estimates of the alloy lifetime are reported in Figure 8. The initial thickness of the alloy is 2 cm. The lifetime was computed as function of the critical vacancy concentration fraction, P_{max}. A passive current density of 5.4×10^{-8} A/cm^2 was selected as input to the model. Lifetimes in Figure 8 are independent of the selected diffusion coefficients (provided that they are less than 10^{-20} cm^2/s), and of the temporal and spatial steps in the finite difference computations. The heuristic model could be improved by accounting for the penetration extent of the corrosion front after active dissolution. As a first approximation, this is accounted by the uncertainty in the model parameter P_{max}.

Assuming stoichiometric and homogeneous dissolution, 5.3×10^{-5} cm/yr, the corrosion rate calculated using Eq. (1) is for a current density of 5.4×10^{-8} A/cm^2. Under this slow corrosion rate, an alloy slab 2 cm thick would fail in 40,000 yr. The failure time of 40,000 yr corresponds to $P_{max} \sim 0.6$ in Figure 8. Values of P_{max} less than 0.6 are not unrealistic, implying shorter lifetimes than those predicted with Eq. (1). Therefore, our analyses show that shorter failure times than those predicted with classic methods are possible.

It is acknowledged that the ideas presented in this paper require experimental verification. Unfortunately, the slow rate of the dissolution process renders verification experiments quite challenging. Accelerated tests at higher temperatures could be attempted bearing in mind that thermodynamics and transport processes at other temperatures may differ. Of particular importance is the verification of the formation of vacancies in the bulk of the alloy. One of the implications of the model is that if the vacancy diffusivity is small (with the consequent accumulation of vacancies at the metal/film interface and negligible vacancy concentration in the bulk of the alloy) then, in the long-term average, alloy dissolution is stoichiometric. In the short term, non-stoichiometric dissolution could be observed such as that revealed in the studies by Cavanaugh et al.[7] However, the non-stoichiometric process cannot be steadily maintained, since that would require fast enough solid-state transport of the preferentially dissolving component. This study evidences that extrapolation of short term behavior (or the order of days, months, years) to long term performance (thousands of years) must be supported by a mechanistic understanding of the dissolution phenomena.

CONCLUSIONS

The passive corrosion rate for Alloy 22, measured in a range of solutions compositions where the pH, chloride

concentration and temperature were varied, was on the order of 5×10^{-5} cm/yr. Preferential dissolution of alloying elements such as Mo, Fe, and Ni was not observed under transpassive conditions The low passive dissolution rate of the alloy suggests that in the absence of localized corrosion, stress corrosion cracking, mechanical failure, or nonstoichiometric dissolution of alloying elements, the lifetime of the containers depends on the passive dissolution rate and the stability of the passive oxide layer. Preliminary modeling calculations also indicate that the preferential dissolution initially observed after exposure is not likely to be sustained.

REFERENCES

1. CRWMS M&O, *Repository Safety Strategy: Plan to Prepare the Postclosure Safety Case to Support Yucca Mountain Site Recommendation and Licensing Considerations*, TDR–WIS–RL–000001, Revision 03, Las Vegas, NV: Office of Civilian Radioactive Waste Management System, Management and Operating Contractor, 2000.

2. P. Marcus, and M. Grimal, Corrosion Science 33(1992): p. 805-814.

3. S. Boudin, J-L. Vignes, G. Lorang, M. Da Cunha Belo, G. Blondiaux, S. M. Mikhailov, J.P. Jacobs, and H. H. Brongersma, Surface and Interface Analysis 22(1994): p. 462-466.

4. S. Haupt, and H.-H. Strehblow, Corrosion Science 37(1995): p.43-54.

5. I. Olefjord, and L. Wegrelius Corrosion Science 31(1990): p.89-98.

6. G. Lorang, N. Jallerat, K. Vu. Quang, and J.-P. Langeron, Surface and Interface Analysis 16(1990): p.325-330.

7. M. A. Cavanaugh, J. A. Kargol, J. Nickerson, and N. F. Fiore, Corrosion 39(1983): p.144-150.

8. W. P. Yang, D. Costa, and P. Marcus, Journal of the Electrochemical Society 141(1994): p.111-116.

9. B. Heine, R. Kirchheim, Corrosion Science 31(1990): p.533-538.

10. R. Kirchheim, B. Heine, H. Fischmeister, S. Hofmann, H. Knote, and U. Stoltz. Corrosion Science 30 (1989): p.899-917.

11. R. Kirchheim, B. Heine, S. Hofmann, and H. Hofsass, Corrosion Science 31(1990): p.573-578.

12. A. Schneider, D. Kuron, S. Hofmann, R Kirchheim, Corrosion Science 31(1990): p.191-196.

13. American Society for Testing and Materials. Standard practice for calculation of corrosion rates and related information from electrochemical measurements: G102–89. *Annual Book of ASTM Standards. Volume 03.02: Wear and Erosion—Metal Corrosion.* West Conshohocken, PA: American Society for Testing and Materials: 416–422. 1999.

14. R.G. Kelly, C.S. Brossia, K.R. Cooper, and J. Krol, J. Chromatography A, 739 (1996): p.191-198.

15. J. Krol, M. Benvenuti, and J. Romano, *Ion Analysis Methods for IC and CIA® and Practical Aspects of Capillary Ion Analysis Theory*, Milford, MA: Waters Corporation (2000).

16. D.S. Dunn, Y.-M. Pan, and G.A. Cragnolino, "Stress Corrosion Cracking, Passive and Localized corrosion of Alloy 22 High-Level Radioactive Waste Containers," CORROSION/2000, paper no. 206 (Houston, TX, NACE International, 2000).

17. O. Pensado and S. Mohanty, "Prediction of waste package life for high-level radioactive waste disposal at Yucca Mountain," *Scientific Basis for Nuclear Waste Management–XXIII*. D. Shoesmith and R. Smith, eds. *Materials Research Society Symposium Proceedings*, Pittsburgh, PA (2000). In press.

18. G.A. Cragnolino, D.S. Dunn, Y.-M. Pan, and O. Pensado, "Corrosion processes affecting the performance of alloy 22 as a high-level radioactive waste container material," *Scientific Basis for Nuclear Waste Management XXIV*. International symposium, August 27 – 31, 2000, Sydney, Australia. Warrendale, PA: Materials Research Society. (2000). To be published.

19. O. Pensado, D.S. Dunn, and G.A. Cragnolino, "Modeling of the Passive Film on Nickel-Chromium-Molybdenum Alloys," Presented at the Symposium on Corrosion of Metals and Alloys, MRS 2000 Spring Meeting. San Francisco, CA, 2000.

20. D. D. Macdonald, Journal of the Electrochemical Society, 139(1992): p.3434-3449.

21. K.E. Heusler. *Passivity of Metals*, edited by R.P. Frankenthal and J. Kruger. The Electrochemical Society, Princeton, NJ, pp. 771-801 (1978).

22. R. Raj and M. F. Ashby, Acta Metallurgica. 23(1975), p.653-666.

23. U.-S. Min and J. C. M. Li, Journal of Materials Research, 9(1994): p.2878-2883.

24. K. Sieradzki, R. R. Coderman, K. Shukla, and R. C. Newman, Philosophical Magazine, 159(1989): p.713-746.

Table 1. Composition of Alloy 22

Ni	Cr	Mo	W	Fe	Co	Mn	Si	S	C	P	V
Bal.	21.60	13.60	3.00	3.80	0.50	0.12	0.030	0.002	0.004	0.008	0.15

Table 2. Results of chemical analyses of test solutions and corrosion product precipitates

Element	Base alloy (wt. percent)	Deposit on specimen (wt. percent)	Deposit on Pt electrode (wt percent)	In solution (wt. percent)
Ni	56.0	6.7	55.0	-
Cr	21.6	22.8	3.9	69.9
Mo	13.6	7.0	4.7	29.1
Fe	3.8	21.3	-	-
W	3.0	18.7	-	-
O	-	21.4	24.3	-

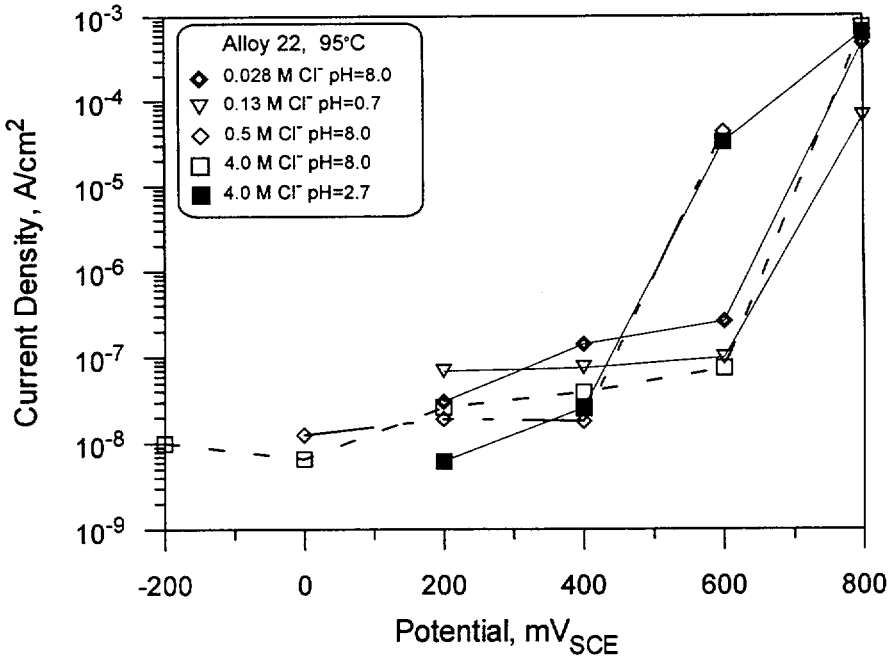

Figure 1. Steady state anodic current densities measured on Alloy 22 under potentiostatic conditions after 48 hr exposure.

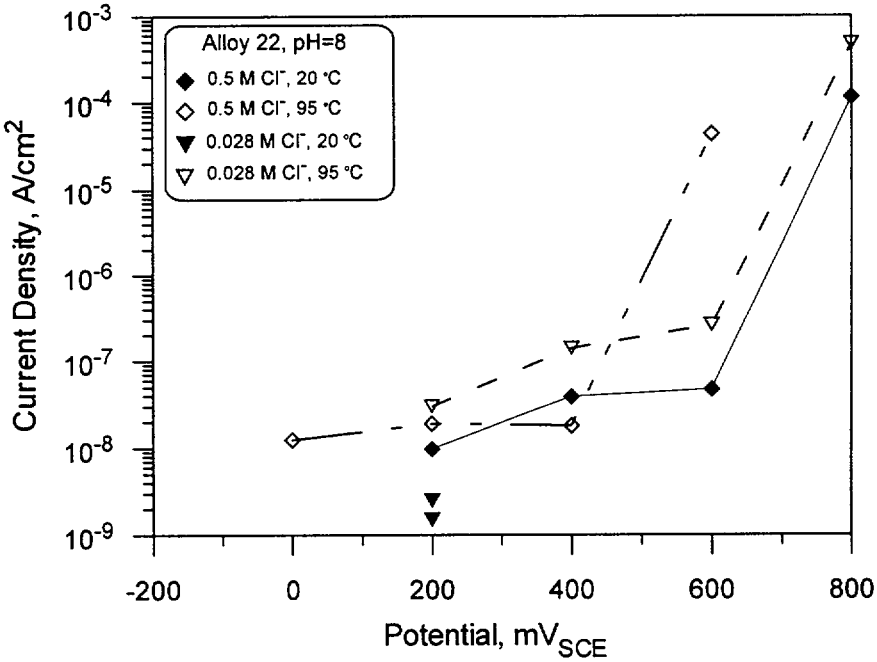

Figure 2. Steady state anodic current densities measured on Alloy 22 as a function of temperature chloride concentration and potential under potentiostatic conditions after 48 hr exposure.

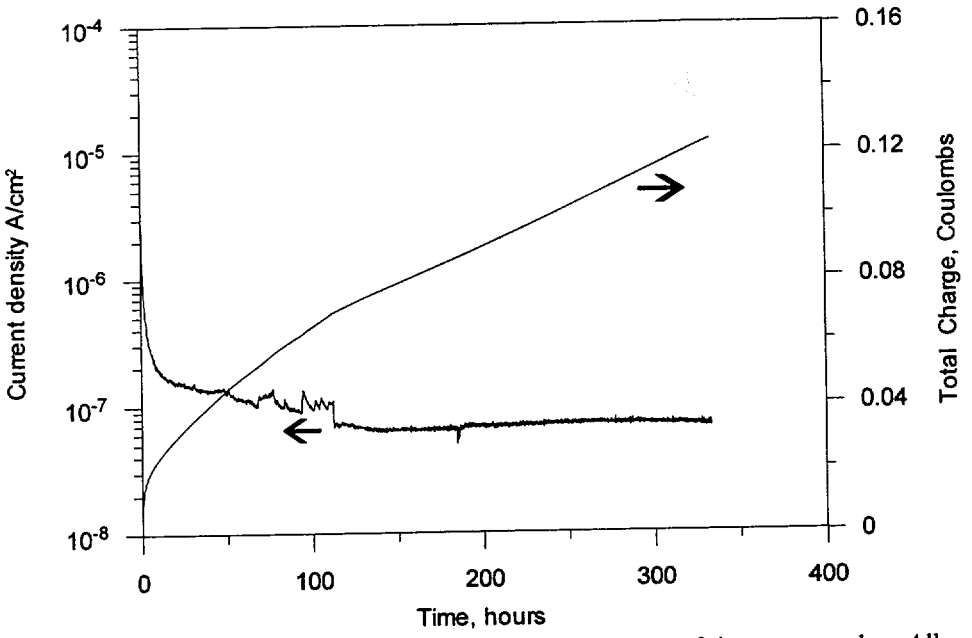

Figure 3. Anodic current density and total charge as a function of time measured on Alloy 22 at 100 mV_{SCE} in 0.028 M chloride solution at 95 °C.

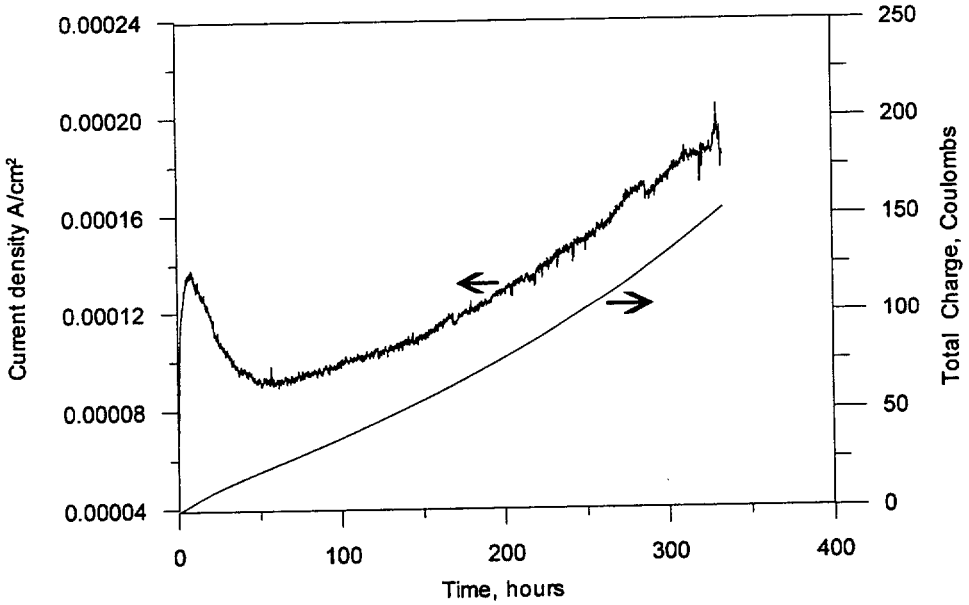

Figure 4. Anodic current density and total charge as a function of time measured on Alloy 22 at 500 mV_{SCE} in 0.028 M chloride solution at 95 °C.

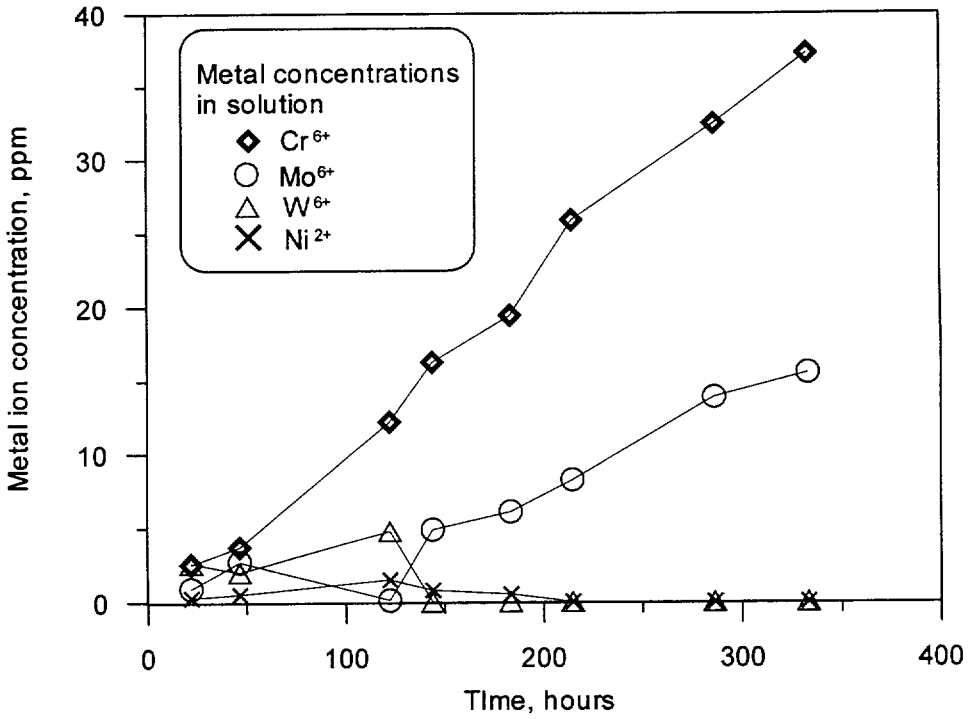

Figure 5. Metal ion concentrations measured using capillary electrophoresis from the anodic dissolution of Alloy 22 at 500 mV_{SCE} in 0.028 M chloride at 95 °C.

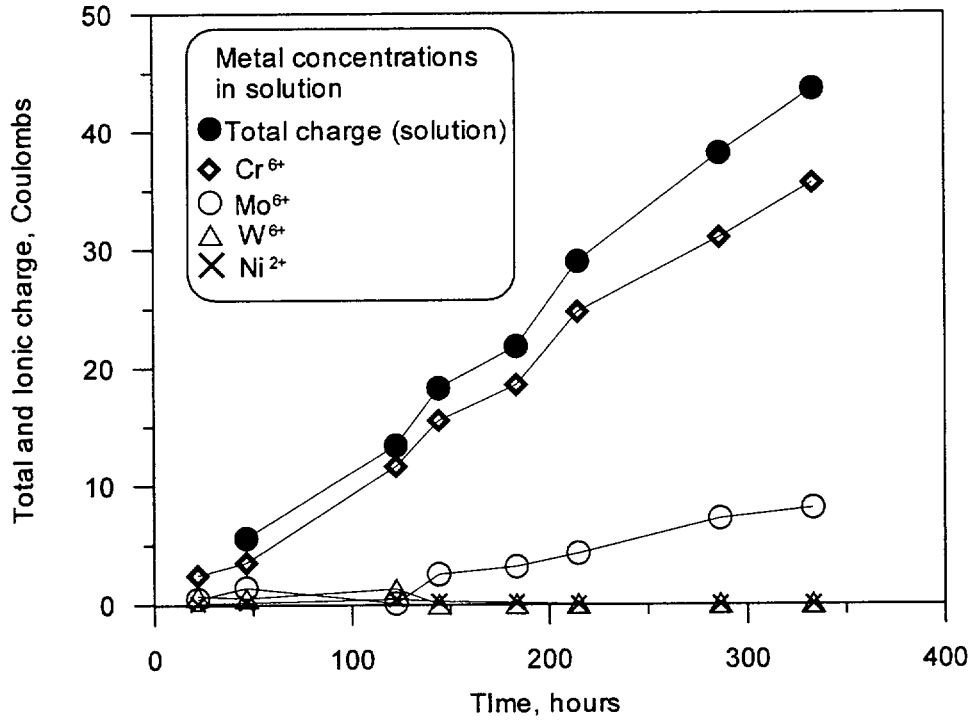

Figure 6. Charge in coulombs for metal ions calculated from the measured solution concentrations. Total charge is the sum of the charge based on solution concentrations.

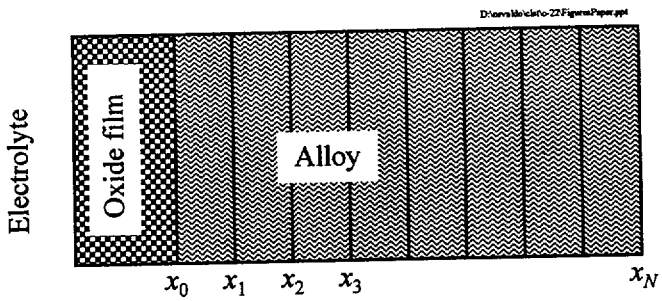

Figure 7: After the fraction of vacancies between x_0 and x_1 exceeds a maximum threshold value, P_{max}, the new metal/film interface is defined to be located at x_1. This process is repeated until the corrosion front penetrates the whole alloy thickness.

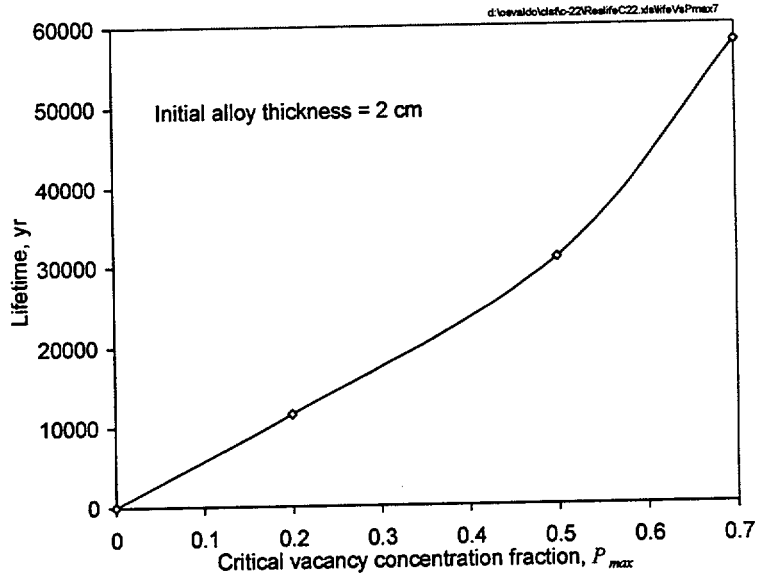

Figure 8: Calculated lifetime of an alloy 22 plate (with an initial thickness of 2 cm) versus the critical vacancy concentration fraction, P_{max}.